Ocean methane hydrates as a slow tipping point in the global carbon cycle

David Archer[a,1], Bruce Buffett[b], and Victor Brovkin[c]

[a]Department of the Geophysical Sciences, University of Chicago, Chicago, IL 60637; [b]Department of the Earth and Planetary Science, University of California, Berkeley, CA 94720; and [c]Max Planck Institute for Meteorology, D-20146 Hamburg, Germany

We present a model of the global methane inventory as hydrate and bubbles below the sea floor. The model predicts the inventory of CH_4 in the ocean today to be ≈1600–2,000 Pg of C. Most of the hydrate in the model is in the Pacific, in large part because lower oxygen levels enhance the preservation of organic carbon. Because the oxygen concentration today may be different from the long-term average, the sensitivity of the model to O_2 is a source of uncertainty in predicting hydrate inventories. Cold water column temperatures in the high latitudes lead to buildup of hydrates in the Arctic and Antarctic at shallower depths than is possible in low latitudes. A critical bubble volume fraction threshold has been proposed as a critical threshold at which gas migrates all through the sediment column. Our model lacks many factors that lead to heterogeneity in the real hydrate reservoir in the ocean, such as preferential hydrate formation in sandy sediments and subsurface gas migration, and is therefore conservative in its prediction of releasable methane, finding only 35 Pg of C released after 3 °C of uniform warming by using a 10% critical bubble volume. If 2.5% bubble volume is taken as critical, then 940 Pg of C might escape in response to 3 °C warming. This hydrate model embedded into a global climate model predicts ≈0.4–0.5 °C additional warming from the hydrate response to fossil fuel CO_2 release, initially because of methane, but persisting through the 10-kyr duration of the simulations because of the CO_2 oxidation product of methane.

clathrate | climate

Large but poorly known amounts of methane are trapped in the sediments beneath the sea floor, frozen into a form of water ice called methane hydrate (1–3). The hydrates could be vulnerable to melting with a deep ocean warming of a few degrees Celsius (3–6), which is obtainable given the available inventories of fossil fuel carbon for combustion. Methane is a greenhouse gas, and it oxidizes in about a decade to CO_2, another greenhouse gas that accumulates in the Earth's carbon cycle and continues to impact climate for many millennia (7, 8). The hydrate carbon reservoir has probably accumulated over millions of years (9, 10), with the gradual cooling of the ocean over geologic time, but a release of carbon from the hydrate pool because of melting could take place on a time scale of millennia (11, 12). Human release of CO_2 from fossil fuel combustion has the potential to make the oceans warmer than they have been in millions of years (13, 14), thus, potentially releasing more methane than the apparently small releases through the repeated glacial-interglacial cycles (15). The methane hydrate reservoir can be considered a slow but, for societal purposes, irreversible tipping point in the Earth's carbon cycle (16).

The melting temperature of hydrate increases with pressure, whereas temperature in the ocean water column decreases with pressure (depth), so in the presence of sufficient concentrations of dissolved methane, hydrate would become increasingly stable with depth in the ocean. However, methane concentrations in the open ocean are too low to support hydrate formation, restricting hydrates to the sediments below the sea floor. Within the sediment column, the temperature increases with depth

(following the geotherm), so that at a depth of a few hundred meters below the sea floor the temperature exceeds the melting threshold. The term "hydrate stability zone" generally refers to the sediment column from the sea floor down to the melting depth, typically a few hundred meters below the sea floor. Climate warming primarily affects hydrate stability near the base of the stability zone, where temperatures approach the melting point. The sediment column provides a thermal buffer that slows the response of the hydrates to climate warming by many centuries.

Much of the methane in ocean hydrate deposits is held in what have been called stratigraphic deposits (17), its concentration determined by the slow processes of sediment accumulation, pore fluid flow, and methanogenesis of buried organic matter. This type of deposit is most amenable to one-dimensional modeling such as we present here. In other deposits, called structural, the methane concentrations are primarily determined by subsurface flow of gaseous methane through faults and porous channels in the sediment column. Structural hydrate deposits can be more concentrated than stratigraphic, and closer to sea floor, making them potentially more responsive to climate warming. Hydrates in the Gulf of Mexico and Hydrate Ridge, for example, are heavily impacted by subsurface gas migration (18–20).

Because much of the hydrate is in stratigraphic deposits, the characteristics of these are used to estimate the total inventory of methane in the ocean. Our estimates of methane release, neglecting structural methane deposits, are likely to be biased severely low for societal time scales of decades to a century. Estimates of the inventory of methane in hydrates range from 700 to 10,000 Pg of C. Uncertainties in the average volume fraction of hydrate accounts for most of this range. Typical values for the average hydrate volume fraction depth-integrated over the stability zone range from 1% to 10% (2, 21–23).

The climate impact of melting hydrates in the ocean depends on whether the carbon reaches the atmosphere in the form of methane. The chemical lifetime of methane in the atmosphere at present concentrations is about a decade, so an abrupt pulse of methane released to the atmosphere would generate a transient spike of high methane concentrations, which would subside in about a decade. If methane is released on a time scale that is long relative to its atmospheric lifetime, the result would be an increase in the steady-state concentration of methane in the atmosphere; a doubling of the total source flux would lead to a bit more than a doubling of the steady-state concentration. The oxidation product of methane is CO_2, another greenhouse gas although a weaker one (per molecule, by a factor of ≈30). In

---

contrast to methane, a transient chemical species, CO_2 accumulates in the atmosphere, ultimately taking hundreds of thousands of years to be consumed by weathering reactions with igneous rocks. Methane that dissolves in the deep ocean would be oxidized to CO_2 (24), in which form it would ultimately equilibrate with the atmosphere, releasing some 15–25% of the carbon to the air.

The bottom-line question is whether the methane released from melting hydrates in the sediment column is likely to escape to the ocean or the atmosphere or to remain in place below the sea floor. The production of bubbles associated with melting may act to destabilize the sediment column to landslides (25). However, even the largest known submarine landslide, the Storrega slide off Norway, did not release a climatically significant amount of methane to the atmosphere (11). The most likely impact of a melting hydrate reservoir is therefore a long-term, chronic methane source, thus, elevating atmospheric methane and contributing to the total CO_2 load on the atmosphere from combustion of fossil fuels.

In the absence of sediment slumping, the sediment column overlying the melting hydrate acts as a physical cap through which the released methane must travel to escape to the ocean or the atmosphere. Assuming that the surface sediment remains colder than the melting temperature, released bubbles or dissolved methane would have to migrate through the cold trap of the stability zone. There is also a chemical trap of oxidation by sulfate. Several authors (10, 26) suggest that the probability of methane escape increases when bubbles make up a large fraction of the pore fluid. High bubble volume would encourage bubbles to migrate through the sediment column by creating a pressure differential between the bubble and the water at the tops and the bottoms of the bubbles. High salinities from freezing hydrate or dissolving evaporates might also create channels of hydrate instability through the nominal stability zone (27–29). Simple kinetics might also allow the methane to escape if it passes through the stability and oxidized zones quickly (30). These mechanisms are motivated, in part, by evidence for free gas moving through the stability zone (31). Mud volcanoes and methane seeps are sometimes lined with frozen hydrate and with $CaCO_3$, the oxidation product of reaction with sulfate, so some fraction of the released gas is clearly captured by the cold and the chemical traps. However, the presence of pockmarks on the sea floor (32) and "wipeout zones" in seismic sections (33) seem to illustrate the potential for methane gas to migrate through the traps to the ocean floor.

Model Descriptions

Hydrate Column Model. We present 2 global models of methane hydrate in the world ocean, one to simulate the detailed spatial distribution of methane and the other to assess its sensitivity to changing climate. Both models are based on the mechanistic 1D methane hydrate sediment column dynamics model developed by Davie and Buffett (9). The model simulates the vertical profiles of methane concentration in its 3 phases (dissolved, gas, and hydrate) within the diffusive/advective framework of the top kilometer of the sediment column. Advection of the pore fluid is assumed to exceed that from compaction by an amount that varies with the sedimentation rate v_s. The magnitude of the interstitial velocity at the seafloor is 1.6 and 1.2 times the flow rate because of sediment compaction in active and passive regions, respectively, with half of the sediment area assumed upward flowing, balanced by another half flowing down. The geothermal gradient is 40 K/km on passive margins and 60 K/km on active margins. The input factors that control the hydrate column model include water depth, temperature, and the depth-dependent rate of methane production, which itself depends on the concentration and reactivity of organic carbon in the sediment. Sedimentary organic carbon is assumed to be converted to
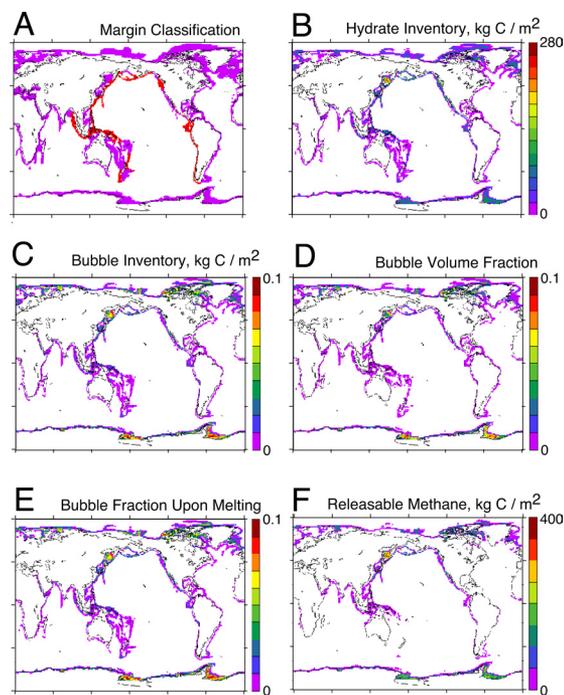
Fig. 1. Maps from the bathymetric model. (*A*) Active (red) versus passive (purple) margin classification. (*B*) Column-integrated inventory of methane in hydrates. (*C*) Column-integrated methane in bubbles. (*D*) Area average bubble fraction of the pore volume. (*E*) Area average bubble fraction upon melting of the hydrate at the base of the stability zone. (*F*) Column inventory of releasable methane, defined as in text.

methane with an efficiency of 25% and a time constant of 3×10^{-13} yr^{-1}. Sediment surface organic carbon concentrations come from the Muds model of the early diagenesis reaction zone (the top meter of the sediment column) (34), which treats the oxic and anoxic diagenesis chemical reactions within a framework of vertical diffusion and sediment accumulation. Kinetic rate parameters in Muds have been tuned by simulated annealing to reproduce field data, including organic carbon concentrations. Muds, in turn, is driven by sediment rain rates to the sea floor, based on fit-to-observed sediment respiration rates as a function of water depth (3) and bottom water oxygen concentrations. The model neglects regional variations in organic carbon rain, such as in river deltas, that may be significant in the real world. To construct a 3D array of model results consisting of 11,520 simulations, the hydrate column model was run to steady state as a function of 3 fundamental driving parameters: water depth (32 values), seafloor temperature (9 values), and bottom water oxygen concentration (40 values). In this study, the hydrate model is applied within the 2 global models by interpolation into the results array according to these parameter values (depth, temperature, and O_2).

Bathymetric Hydrate Distribution Model. Maps of hydrate distribution were constructed by using the 2-min gridded ETOPO2 global bathymetry and the Levitus *et al.* (35) gridded ocean climatologies (Fig. 1). At each grid point in the bathymetry, the water temperature and oxygen concentration are interpolated from the Levitus fields. The margin is classified into active and passive regions for purposes of fluid flow as in Fig. 1*A*. The hydrate model results are interpolated from the 3D results array described above. The results from the high-resolution ETOPO2 grid are summed into a $1° \times 1°$ grid for presentation. The hydrate distribution model is conceptually similar to the binned model
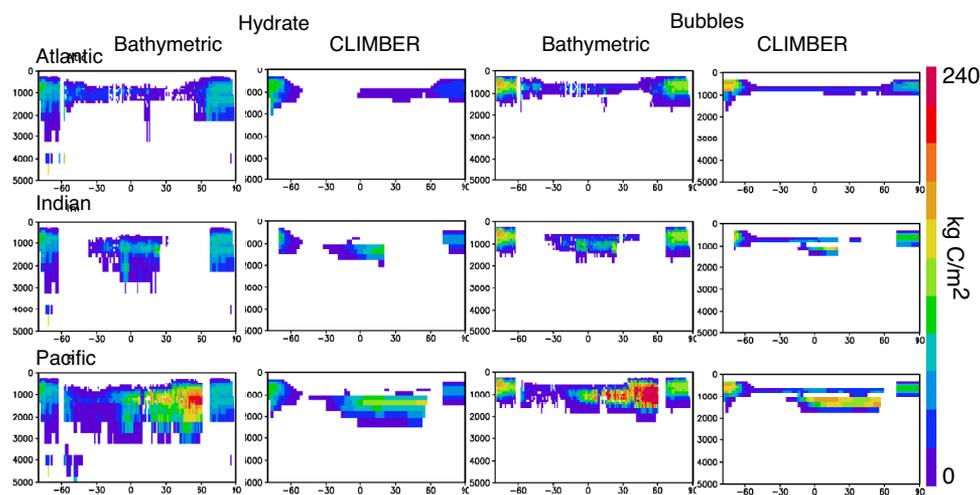
Fig. 2. Depth/latitude sections of methane distribution, from the bathymetric model and from CLIMBER.

described in ref. 3, but here the distribution of hydrate is cast into a geographical context.

Model of Hydrates in Global Climate. We assess the climate sensitivity of ocean hydrates by using the climate system model CLIMBER-2 (36, 37). The model includes a 2.5-dimensional, statistical-dynamical atmosphere with a coarse spatial resolution of 10° in latitude and 51° in longitude. The ocean consists of 3 zonally averaged basins with a latitudinal resolution of 2.5° and 20 unequal vertical levels. The ocean carbon cycle model includes an oceanic biogeochemistry model with phosphate-limited biota (38) and a deep-ocean carbonate sediment model (39). The model is constructed to simulate the interactions between carbon and climate on multimillennial time scales (40). The land surface model was not allowed to release or take up carbon in these simulations because of the large uncertainties in land use changes that could take place in the near future and, in the long term, the ocean has the capability to store more CO_2 than the land surface could. The CLIMBER model has a climate sensitivity and transient response which is comparable with full primitive equation models, according to model intercomparisons for the past (41) and future (42) climates, as well as intercomparisons of coupled climate-carbon cycle models (43).

Hydrates were added to CLIMBER by using the same matrix of model results as was used in the bathymetric model. ETOPO5 bathymetry was used to calculate the sea floor area associated with each ocean grid point in CLIMBER. An initial steady state used the CLIMBER temperature and oxygen fields to find a steady-state methane inventory for the location. As the ocean temperature evolves in a time-dependent simulation, the temperature is used to calculate what the steady-state methane inventory would be. A time-evolving methane steady-state inventory is computed by relaxation toward the full steady state with a time constant of 1,000 yr. This time lag is necessary to account for the slow process of heat diffusion into the sediment column. The actual release of methane is determined by whether the bubble volume upon melting exceeds an assumed critical bubble fraction, as described in *Simulation of the Climate Sensitivity of Ocean Hydrate*. After the initial spin-up, changes in the ocean oxygen concentrations are not allowed to impact the hydrate inventory because it takes millions of years for surface sediment to reach the methanogenesis zone. Similarly, we do not allow a buildup of methane in response to cooling, as in the period after the peak warming, because it takes millions of years for methanogenesis to supply methane. In one scenario, methane is oxidized to CO_2 in the water column, consuming oxygen and

provoking $CaCO_3$ dissolution, and in the other, the methane decomposes to CO_2 in the atmosphere with a time constant of 10 yr.

Simulation of the Distribution of Ocean Hydrate

Maps of methane inventory and characteristics from the bathymetric distribution model are shown in Fig. 1. The inventories of methane hydrate (Fig. 1*B*) are comparable to those of bubbles (Fig. 1*C*). The average bubble volume fraction of the pore space is shown in Fig. 1*D*, and Fig. 1*E* shows the bubble volume fraction predicted by the model if the hydrate at the base of the stability zone were to melt. Sections of methane inventory in depth and latitude are compared in Fig. 2 between the bathymetric model, by binning the results zonally, and CLIMBER, in which the ocean is formulated in the zonal mean. The 2 global models are each based on the same hydrate column model so it is no surprise that their methane distributions correspond well.

The global inventory of methane is 1,700 Pg of C, 3-fold smaller than the result we published with the binned version of the model (3). Most of the difference, it must be admitted, was because of an interpolation error affecting the bathymetry of some very deep parts of the ocean. Some of the change is because of other factors such as the elimination of places (i.e., midocean ridges) that are shallow enough for the depth-bin scheme to pick up as containing hydrate but are too far from shore to get the high organic carbon rains typical of nearshore environments (and assumed in the depth-dependent organic carbon rain input to the model). The total methane inventory in CLIMBER is ≈2,000 Pg of C, which is ≈25% higher than in the high-resolution model. The methane inventories may differ between the 2 models if the temperature or the oxygen concentrations are not exactly the same.

From the bathymetric model, we show several sensitivity cases in addition to the default or "Full" model. The uniform temperature case (labeled "T") used a depth-dependent but horizontally averaged temperature profile rather than taking the spatially varying temperature from Levitus *et al.* (35). Uniform oxygen (labeled "O_2") does the same for O_2. The third sensitivity study gauged the importance of the distinction between active and passive margins, which affects the rate of pore fluid flow in the model. All of the marginal area is taken to be active in this case (labeled "Active"). The methane distributions from both global models are binned according to basin in Fig. 3 and according to water depth in Fig. 4.

In both global models, there is far more methane stored in the Pacific than in the Atlantic Ocean. This can be seen most
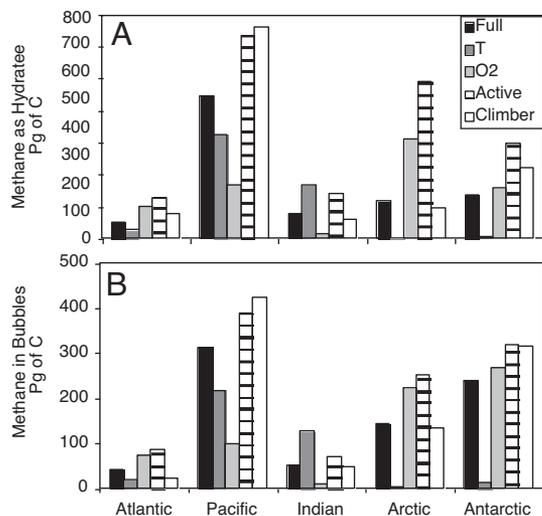
Fig. 3. Basin inventories of methane in hydrate (*A*) and bubbles (*B*). There are 4 versions of the bathymetric model (the full-default configuration and 3 sensitivity studies: uniform T, uniform O_2, and all active margin type) and CLIMBER.

explicitly in Fig. 3 but is also obvious to the eye from Figs. 1 and 2. In the bathymetric simulation, the Pacific contains nearly 10 times more methane than the Atlantic. There are several potential sources of heterogeneity in the hydrate distribution: (*i*) deep ocean temperatures, (*ii*) oxygen concentrations, which determine organic carbon preservation in our model, and (*iii*) differences in pore fluid advection, addressed in our model by the distinction between "active" and "passive" areas.

The impact of each source of heterogeneity can be assessed from the 3 sensitivity studies. The Pacific has most of the area of the sea floor classified in our model as "active" rather than "passive" margin, resulting in some enhancement of the Pacific methane inventory. However, the uniform-oxygen study shows that the main reason for higher Pacific methane storage is its lower oxygen concentrations, leading to enhanced preservation of organic carbon. This is an unfortunate sensitivity to discover in the model because oxygen concentrations today might not be typical of the oxygen distributions millions of years ago when the organic carbon supplying methanogenesis today was first deposited. We regard the difference between the full model and the uniform-oxygen model an indication of the uncertainty in pre-
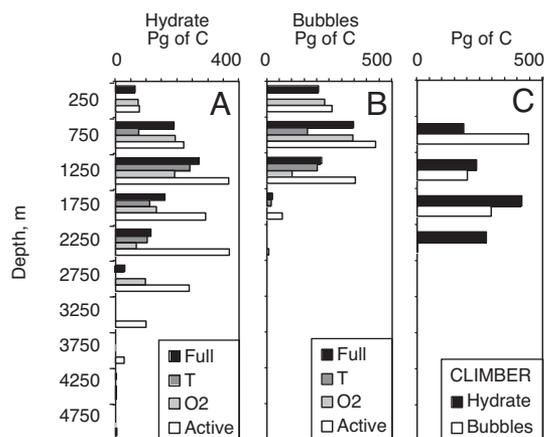
Fig. 4. Depth distribution of methane in hydrates (*A*) and bubbles (*B*) from the bathymetric model, and from CLIMBER (*C*).
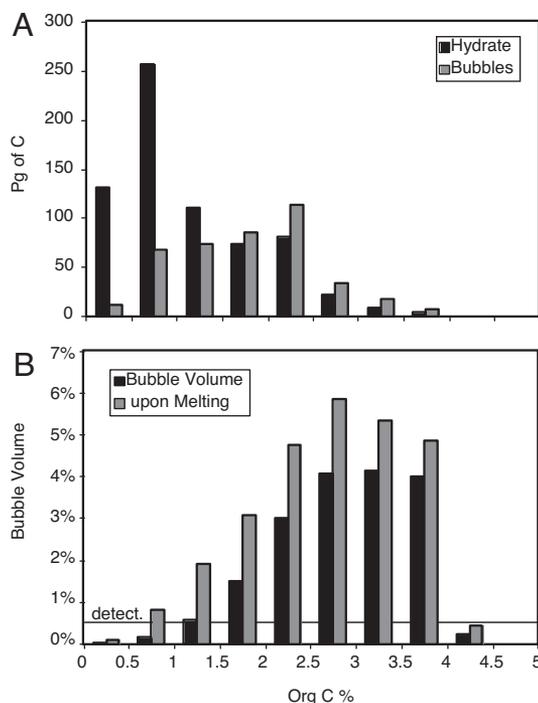
Fig. 5. Results from the bathymetric model. (*A*) Methane inventories binned according to the organic carbon content of the surface sediment. (*B*) Bubble volumes averaged in bins of organic carbon content. The line labeled "detect." indicates a 0.5% seismic delectability threshold.

dicting hydrate distributions by using surface sediments as a predictor for the dynamics of methane below.

The uniform-temperature "T" sensitivity study shows the importance of temperature for methane storage in the high-latitude Arctic and Antarctic regions. The colder water column in the high-latitude ocean also allows methane to accumulate in shallower water depths than is possible elsewhere, as can be seen in the depth distribution of methane hydrate and bubbles in Fig. 4. The uniform-temperature simulation eliminates all accumulation of methane shallower than 500 m, and the inventory in the top kilometer drops by a factor of 3. Hydrate in shallower water depths is important for the forecast because it will be reached by climate warming soonest and most strongly. These regions are located in high latitudes where climate warming is supposed to be the most intense.

The inventories of methane as hydrate and bubbles are binned according to the organic carbon content of the sediment in Fig. 5. As observed in the real ocean, bubbles are typically not found when organic carbon concentrations drop below 1% (Fig. 5*B*). In the model, methane hydrate accumulates at lower organic carbon concentration so that most of the inventory globally is found in sediments in the 0.5–1% organic carbon content bin. If this is true in the real world, it would mean that hydrate might exist over a much wider area of the sea floor than previously thought.

Simulation of the Climate Sensitivity of Ocean Hydrate

The steady-state inventory of methane in both global models exhibits a similar sensitivity to uniform offsets of the temperature of the ocean, as did its predecessor model (3). A warming of 3 °C is sufficient to reduce the steady-state inventory by more than half in either model (Fig. 6).

The big unknown for predicting the future evolution of the methane is how much of it will escape the sea floor to reach the ocean or the atmosphere. We have tried to scale the problem by

Fig. 6. Sensitivity of the total ocean inventory of methane from hydrates plus bubbles to uniform changes in ocean temperature, from the bathymetric model and from CLIMBER.

considering the volume fraction of the pore space that is occupied by bubbles if the hydrate at the base of the stability zone were to melt. The idea is that at some critical bubble fraction, the bubbles begin to interconnect and migrate through the sediment column. The calculation begins with the equilibrium methane inventory at the present-day temperature of the ocean. We compute also the bubble volume that would be generated if the hydrate at the present-day base of the stability zone were to melt. When the sediment column warms, if the bubble volume upon melting exceeds a critical value, then the sediment column is allowed to release enough methane to bring it to its warmer steady-state inventory. If the bubble volume upon melting does not exceed critical, the methane is retained in the sediment column. We call this quantity "releasable methane." Using the bathymetric model, we computed the amount of releasable methane in equilibrium as a function of a spatially uniform temperature increase. A map of this methane distribution in response to 3 °C of warming is shown in Fig. 1*F*. Results from a range of different warming scenarios and assumed critical bubble volume fractions are shown in Fig. 7. Assuming a 10% critical bubble fraction for gas escape (44), the bathymetric model predicts that only 2% of the methane inventory (≈30 Pg of C) would escape in response to 3 °C of warming.

However, we expect the hydrate column model to systematically underestimate the amount of methane in high concentration deposits. Selective deposition of hydrate in sandy sediments would increase the hydrate concentration there. Gas migration may be facilitated by faults and channels in the sediment column. The structural deposits that are omitted in our model formulation probably contain higher concentrations of bubbles and would be more likely to release methane to the sea floor. The model estimate is therefore a conservative representation of a large fraction of the methane, presumably, but not the most

Fig. 7. Amount of methane released by the bathymetric model as a function of a uniform change in ocean temperature (*x* axis), and the value of the critical bubble fraction enabling gas escape from the sediment column (symbols as indicated in the figure).

Fig. 8. Transient response of the ocean methane hydrate reservoir within the CLIMBER model subjected to fossil fuel CO_2 forcing of 1,000 and 5,000 Pg of C. The model assumes a critical bubble fraction of 2.5%.

volatile fraction of the methane. If we compensate for the model bias toward homogeneity by decreasing the model critical bubble fraction that we assume, a critical bubble volume of 2.5% would be small enough to predict the loss of more than half of the methane given a warming of 3 °C.

The time evolution of ocean hydrates is simulated by using the CLIMBER model in Fig. 8. The model was subjected to CO_2 emission scenarios of moderate scale (1,000 Pg of C) and large scale (5,000 Pg of C) taken from ref. 8. Simulations without methane release are labeled as Fossil Fuels in Fig. 8. For each emission scenario, 2 extreme scenarios are considered; one with complete methane oxidation and consequent CO_2 dissolution in the water column (hydrates as CO_2), and the other assumes that the released methane reaches the atmosphere, where it oxidizes to CO_2 with a 10-yr time constant (hydrates as CH_4). In the later scenario, the radiative effect of methane is calculated in terms of an equivalent CO_2 concentration following Shin *et al.* (45).

The model ultimately releases 450 Pg of C in methane in response to 1,000 Pg of C from fossil fuels, or 600 Pg of C in methane after 5,000 Pg of C from fossil fuels. We reiterate that the magnitude of methane release depends fundamentally on the critical bubble volume for gas escape from the sediment column, a parameter that is largely a poor constraint for the real world and poorly simulated by the model, for reasons explained above. For the first few thousand years of the simulations, the climate impact of the melting hydrate depends on whether methane gas reaches the atmosphere. Methane is released over a time period of several thousand years, warming the atmosphere by ≈0.4– 0.5 °C in response to either fossil fuel CO_2 release scenario. As the excess methane concentration decreases after a few thousand years, the accumulated CO_2 from methane oxidation, either in the ocean or in the atmosphere, acts to perpetuate a warming of about this same magnitude for the entire 10-kyr duration of the simulations.

A warming of 2 °C is often taken as a benchmark for "dangerous anthropogenic interference in the climate system" (46). The moderate fossil fuel emission scenario (1,000 Pg of C) without hydrates comes close to this warming at the time of the CO_2 peak, but the warming quickly subsides as CO_2 dissolves in the ocean. The impact of hydrates oxidized to CO_2 in the ocean is to prolong the period of near-peak warming for thousands of years, by the gradual release of carbon from the ocean. If the methane reaches the atmosphere, the additional warming from the methane puts the temperature significantly over the 2 °C

benchmark, also for thousands of years. The simulation is not really a forecast because of the uncertainty in the mechanism for methane release but rather a demonstration of the potential for ocean hydrates to impact the severity of anthropogenic global warming on long time scales.

Conclusions

The modeling of methane hydrate is frankly in its infancy, and several factors of first-order importance are only crudely represented. The results of this paper should be regarded as a progress report rather than as a definitive statement about the methane cycle in the real ocean. That being said, it seems robust to conclude, based on this study and others (47), that mankind has the capacity (given our fossil fuel resources) to ultimately melt a significant fraction of the methane hydrates in the ocean.

It also seems clear that the climate impacts of this would be primarily on time scales of millennia and longer. The methane hydrates in the ocean seem precarious, unstable to buoyancy, unstable to melting, and unstable to chemical reactions, but no one has thought of a mechanism that would release a significant fraction of the methane in the ocean on a human time scale of the coming century. A more plausible scenario would be a slow, chronic release of methane from ocean hydrates comparable to the release from high-latitude peats, for example (48). Because the ocean methane hydrates comprise a large pool of potentially releasable carbon, they have the potential to have a strong, long-term impact on Earth's climate.

1. Kvenvolden KA (1993) Gas Hydrates - Geological Perspective and Global Change. *Rev Geophys* 31:173–187.
2. Milkov AV (2004) Global estimates of hydrate-bound gas in marine sediments: How much is really out there? *Earth-Sci Rev* 66:183–197.
3. Buffett B, Archer DE (2004) Global inventory of methane clathrate: Sensitivity to changes in the deep ocean. *Earth Planet Sci Lett* 227:185–199.
4. Dickens GR, O'Heill JR, Rea DK, Owens RM (1995) Dissociation of oceanic methane hydrate as a cause of the carbon isotope excursion at the end of the Paleocene. *Paleoceanography* 19:965–971.
5. Kennett JP, Cannariato KG, Hendy IL, Behl RJ (2000) Carbon isotopic evidence for methane hydrate instability during quaternary interstadials. *Science* 288:128–133.
6. Nisbet EG (1992) Sources of atmospheric CH_4 in early postglacial time. *J Geophys Res* 97:12859–12867.
7. Archer, D (2005) Fate of fossil-fuel CO_2 in geologic time. *J Geophys Res* 110:C09S05.
8. Archer D, Brovkin, V (2007) The millennial lifetime of fossil fuel CO_2. *Climatic Change* 90:283–297.
9. Davie MK, Buffett BA (2001) A numerical model for the formation of gas hydrate below the seafloor. *J Geophys Res* 106:497–514.
10. Dickens, G. R (2001) in *Natural Gas Hydrates: Occurance, Distribution and Detection* (American Geophysical Union, Washington, DC), Vol 124, pp 19–38.
11. Archer DE (2007) Methane hydrate stability and anthropogenic climate change. *Biogeosciences* 4:993–1057.
12. Kennett JP, Cannariato KG, Hendy IL, Behl RJ (2003) *Methane Hydrates in Quaternary Climate Change: The Clathrate Gun Hypothesis* (American Geophysical Union, Washington, DC).
13. Stouffer RJ, Manabe S (2003) Equilibrium response of thermohaline circulation to large changes in atmospheric CO_2 concentration. *Climatic Dyn* 20:759–773.
14. Martin PA, et al. (2002) Quaternary deep sea temperature histories derived from benthic foraminiferal Mg/Ca. *Earth Planet Sci Lett* 198:193–209.
15. Sowers T (2006) Late quaternary atmospheric CH_4 isotope record suggests marine clathrates are stable. *Science* 311:838–840.
16. Dickens GR (2003) Rethinking the global carbon cycle with a large, dynamic and microbially mediated gas hydrate capacitor. *Earth Planet Sci Lett* 213:169–183.
17. Milkov AV, Sassen R (2002) Economic geology of offshore gas hydrate accumulations and provinces. *Mar Petrol Geol* 19:1–11.
18. Sassen R, et al. (2001) Massive vein-filling gas hydrate: Relation to ongoing gas migration from the deep subsurface in the Gulf of Mexico. *Mar Petrol Geol* 18:551–560.
19. Torres ME, et al. (2002) Fluid and chemical fluxes in and out of sediments hosting methane hydrate deposits on Hydrate Ridge, OR, I: Hydrological provinces. *Earth Planet Sci Lett* 201:525–540.
20. Shipley, T. H (1979) Seismic reflection evidence for the widespread occurrence of possible gas-hydrate horizons on continental slopes and rises. *AAPG Bull* 63:2204–2213.
21. Kvenvolden KA (1995) A review of the geochemistry of methane in natural gas hydrate. *Org Geochem* 23:992–1008.
22. Dickens GR (2001) The potential volume of oceanic methane hydrates with variable external conditions. *Org Geochem* 32:1179–1193.
23. Holbrook WS, et al. (1996) Methane hydrate and free gas on the Blake Ridge from vertical seismic profiling. *Science* 273:1840–1843.
24. Valentine DL, Blanton DC, Reeburgh WS, Kastner M (2001) Water column methane oxidation adjacent to an area of active hydrate dissociation, Eel River Basin. *Geochim Cosmochim Acta* 65:2633–2640.
25. Kayen RE, Lee HJ (1991) Pleistocene slope instability of gas hydrate-laden sediment of Beaufort Sea margin. *Mar Geotech* 10:125–141.
26. Flemings BP, Liu X, Winters WJ (2003) Critical pressure and multiphase flow in Blake Ridge gas hydrates. *Geology* 31:1057–1060.
27. Liu XL, Flemings PB (2006) Passing gas through the hydrate stability zone at southern Hydrate Ridge, offshore Oregon. *Earth Planet Sci Lett* 241:211–226.
28. Milkov AV, et al. (2004) Co-existence of gas hydrate, free gas, and brine within the regional gas hydrate stability zone at Hydrate Ridge (Oregon margin): Evidence from prolonged degassing of a pressurized core. *Earth Planet Sci Lett* 222:829–843.
29. Ruppel C, Dickens GR, Castellini DG, Gilhooly W, Lizarralde, D (2005) Heat and salt inhibition of gas hydrate formation in the northern Gulf of Mexico. *Geophys Res Lett* 32:L04605.
30. Cathles LM, Chen DF (2004) A compositional kinetic model of hydrate crystallization and dissolution. *J Geophys Res* 109:B08102.
31. Holbrook WS, et al. (2002) Escape of methane gas through sediment waves in a large methane hydrate province. *Geology* 30:467–470.
32. Hovland M, Judd AG (1988) *Seabed pockmarks and seepages* (Graham and Trotman, London).
33. Hill JC, Driscoll NW, Weissel JK, Goff JA (2004) Large-scale elongated gas blowouts along the US Atlantic margin. *J Geophys Res* 109:B09101.
34. Archer DE, Morford JL, Emerson SR (2002) A model of suboxic sedimentary diagenesis suitable for automatic tuning and gridded global domains. *Global Biogeochem Cycles* 16:1017.
35. Levitus S, Conkright ME, Reid JL, Najjar RG, Mantyla A (1993) Distribution of nitrate, phosphate, and silicate in the world's oceans. *Prog Oceanogr* 31:245–273.
36. Ganopolski A, et al. (2001) CLIMBER-2: A climate model of intermediate complexity. Part II: Model sensitivity. *Climate Dyn* 17:735–751.
37. Petoukhov V, et al. (2000) CLIMBER-2: A climate system model of intermediate complexity. Part I: Model description and performance for present climate. *Climate Dyn* 16:1–17.
38. Brovkin V, et al. (2002) Carbon cycle, vegetation and climate dynamics in the Holocene: Experiments with the CLIMBER-2 model. *Global Biogeochem Cycles* 16:1139.
39. Archer DE (1991) Modeling the calcite lysocline. *J Geophys Res* 96:17037–17050.
40. Brovkin V, Ganopolski A, Archer D, Rahmstorf S (2007) Lowering of glacial pCO_2 in response to changes in oceanic circulation and marine biogeochemistry. *Paleoceanography* 22:PA4202.
41. Weber SL, et al. (2007) The modern and glacial overturning circulation in the Atlantic ocean in PMIP coupled model simulations. *Climate Past* 3:51–64.
42. Petoukhov V, et al. (2005) EMIC Intercomparison Project (EMIP-CO_2): Comparative analysis of EMIC simulations of climate, and of equilibrium and transient responses to atmospheric CO_2 doubling. *Climate Dyn* 25:363–385.
43. Friedlingstein P, et al. (2006) Climate-carbon cycle feedback analysis: Results from the C4MIP-model intercomparison. *J Climate* 19:3337–3353.
44. Flemings PB, Stump BB, Finkbeiner T, Zoback M (2002) Flow focusing in overpressured sandstones: Theory, observations, and applications. *Am J Sci* 302:827–855.
45. Shin SI, et al. (2003) A simulation of the Last Glacial Maximum using the NCAR-CCSM. *Climate Dynamics* 20:127–151.
46. Grassl H, et al. (2003) *Climate Protection Strategies for the 21st Century: Kyoto and Beyond* (German Advisory Council on Global Change, Berlin), pp 1–89.
47. Reagan MT, Moridis GJ (2007) Oceanic gas hydrate instability and dissociation under climate change scenarios. *Geophys Res Lett* 34:L22709.
48. Walter KM, Zimov SA, Chanton JP, Verbyla D, Chapin FS (2006) Methane bubbling from Siberian thaw lakes as a positive feedback to climate warming. *Nature* 443:71–75.

SUSTAINABILITY SCIENCE

GEOPHYSICS